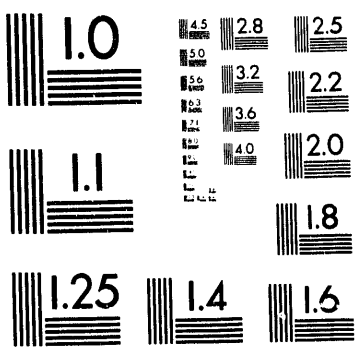
1.0
1.1
1.25
1.4
1.6
1.8
2.0
2.2
2.5
2.8
3.2
3.6
4.0
4.5
5.0
5.6
6.3
7.1

1 of 1

Chemical Reaction Fouling Model for Single-Phase Heat Transfer

C. B. Panchal
Argonne National Laboratory
Argonne, Illinois 60439

A. P. Watkinson
University of British Columbia
Vancouver, B. C., V6T 1Z4, Canada

This paper is being submitted for presentation at the 29th ASME/AIChE National Heat Transfer Conference, August 1993, Atlanta

Chemical Reaction Fouling Model for Single-Phase Heat Transfer*

C. B. Panchal
Argonne National Laboratory
Argonne, Illinois 60439

A. P. Watkinson
University of British Columbia
Vancouver, B. C., V6T 1Z4, Canada

ABSTRACT

A fouling model was developed on the premise that the chemical reaction for generation of precursor can take place in the bulk fluid, in the thermal-boundary layer, or at the fluid/wall interface, depending upon the interactive effects of fluid dynamics, heat and mass transfer, and the controlling chemical reaction. The analysis was used to examine the experimental data for fouling deposition of poly-peroxides produced by autoxidation of indene in kerosene. The effects of fluid and wall temperatures for two flow geometries were analyzed. The results showed that the relative effects of physical parameters on the fouling rate would differ for the three fouling mechanisms; therefore, it is important to identify the controlling mechanism in applying the closed-flow-loop data to industrial conditions.

INTRODUCTION

Organic-fluid fouling is a costly problem for the chemical, petrochemical, and other industries which process organic chemicals. In general, insoluble foulants are formed by chemical reactions between reacting species present in the process stream. The interactive effects of the chemical reactions, fluid dynamics, and heat/mass transfer mechanisms make understanding of the fouling process quite difficult. The presence of particulate matter, inorganic salts, and incompatible species alters the overall deposition process, but the chemical reaction is the governing process. A critical review of organic-fluid fouling by Watkinson [1] summarized the present state of knowledge in this field and identified a number of key technical areas. One such area is the mathematical description of foulant formation followed by deposition

---

*Work supported by the U. S. Department of Energy, Assistant Secretary for Conservation and Renewable Energy, Office of Industrial Technology, Office of Industrial Processes, under contract W-31-109-Eng-38.

on the heat-exchange surface. A mechanistic description of the fouling process is essential to identify the controlling mechanism(s) and determine the effects of physical parameters. It may not be possible to develop a detailed chemical-reaction model for many complex fluid systems; however, a basic fouling model would be a useful tool to identify the rate-controlling step, thereby facilitating the application of laboratory data to industrial conditions. The fouling model can serve as an analytical tool for determining the interactive effects of the chemical and physical processes associated with organic-fluid fouling.

Since the model proposed by Kern and Seaton [2], several investigators have formulated fouling models on the basis of assumptions governing a particular fouling problem. Crittenden [3] provided a general review of models for chemical-reaction fouling, including corrosion fouling. Some of the selected analyses that are applicable to organic-fluid fouling, along with assumptions used by the investigators, are shown in Table 1. These models were used to correlate a particular set of experimental data; therefore, they may lack characteristics of a model required to identify the controlling mechanism. Some of these models did not include the time-dependent generation of precursor in a closed-flow-loop experimental apparatus. As a result, application of these models to other experimental systems and industrial processes would introduce an unknown level of uncertainty. The models assumed reaction of a single species, usually by first order kinetics. The models generally lacked flexibility to be usefully applied to complex experimental systems or to industrial situations.

Table 1. Summary of Fouling Models

Investigator	Basic Assumptions
Nijsing [4]	Instantaneous first-order reaction at wall surface Diffusion term included Rapid deposition of foulant
Watkinson et al. [5]	Precursor present in bulk Insoluble foulant formed in bulk Sticking inversely proportional to velocity
Crittenden et al. [6]	Precursor present in bulk Foulant formation occurred at wall surface Finite solubility of foulant Back-diffusion of foulant
Paterson et al. [7]	Zero-order reaction kinetics No mass diffusion resistance

In the present analysis, a generalized approach was taken to describe the interactive effects of the controlling chemical reaction and transport processes. The analysis included only the initial deposition and did not consider removal or the film-aging process. The latter is governed by the reaction in the fouling film at the wall temperature; therefore, the effects of fluid dynamics would be minimal and it could be system-specific. The mathematical model followed an approach commonly used for tubular chemical reactors; however, major emphasis was placed on the transport processes and on reactions occurring near the wall surface. The model was kept as general as possible so that fouling mechanisms with different chemical kinetics can be easily analyzed. It is understood that the mathematical model introduces physical parameters (e.g., diffusion coefficient of a species) that are difficult to estimate; however, many such parameters can be lumped together to evaluate their relative effects. In order to illustrate the fouling model, the predicted results for deposition of poly-peroxide of indene were compared with the experimental data obtained at Argonne National Laboratory by using an in-tube flow monitor and at the University of British Columbia by using an annular flow monitor.

PHYSICAL MODEL

The physical model in the present analysis is based on the assumption that the key chemical reaction can be expressed in a two-step reaction: generation of soluble precursor followed by formation of insoluble foulant.

Reactants	------>	Precursor	----->	Foulant
(soluble)	r_1	(sparingly soluble)	r_2	(insoluble)

The critical review by Watkinson [1] showed that in many cases, in particular for hydrocarbons, the complex reaction associated with the fouling process can be simplified to a two-step reaction. The heat-exchange equipment operates with finite heat fluxes, and the kinetic constant for a given chemical reaction is a strong function of local temperature; therefore, the fouling model must include the effects of temperature gradient near the wall surface. The interactive effects of chemical reaction, mass diffusion, fluid dynamics, and temperature distribution can produce three fouling cases which are differentiated on the basis whether generation of precursor occurs, in the bulk fluid, in the thermal boundary layer, or at the wall surface. Figure 1 is a schematic diagram of the physical model. The Case 1 and Case 2 models can be further divided depending upon whether the second reaction occurs in the bulk fluid or in the thermal-boundary layer. If insoluble foulant formation occurs in the bulk for Case 1, the subsequent fouling process should be treated as particulate fouling. Because the thermal-

boundary layer is relatively thin, it should be appropriate to assume that the foulant formed in the thermal boundary layer is deposited on the wall surface; therefore, the case 2 mechanism is not divided into two subcases.

The model represented by Figure 1 can be used to predict the effects of operating variables on the fouling processes. Predictions can then be compared with the experimental results to help elucidate the controlling mechanism. Once the governing mechanism is identified, the physical model should help in determining threshold fouling conditions and applying the laboratory data to industrial conditions. Moreover, the model should help to make an effective use of antifouling chemicals, and hence reduce the use of such chemicals. The present model is a first step toward the development of a comprehensive fouling model for hydrocarbons, in which the effects of particulates, inorganic salts, and the presence of such complex substances as asphaltene are included. With the help of the model, it should be possible to explain the fouling behavior of some heat-exchange units, where precursor is carried from one unit to another unit, or is generated in the process equipment (e.g., reactor).

MATHEMATICAL MODEL

The fouling loop consists of a feed tank, piping, and the heat-transfer test section. The tank is treated as a well mixed vessel, and for the heat-transfer section, the model is based on the microscopic balances for turbulent flow in a tube using the maximum gradient approach of Himmelblau and Bischoff [8]. The flow is considered to be one-dimensional, and axial dispersion is neglected. The generation of fouling species by reaction, and their transport to the boundary of the control volume, is described below. The first reaction of the two-step fouling process is described in terms of two reactants with reaction order m and n. This expression is applicable to autoxidation of olefins as indicated by the experimental work of Russell [10].

$$r_1 = k_1 Cr_1^m \quad Cr_2^n \qquad (1)$$

The second reaction is expressed in terms of precursor concentration only.

$$r_2 = k_2 C_p^l \qquad (2)$$

The reaction rate constants k_1 and k_2 have the Arhenius form.

$$k_j = A_j \exp(-E_j/RT) \qquad (3)$$

In the following section, equations are formulated for calculating the local rate of fouling for each of the three fouling mechanisms. These equations are then combined with the heat- and mass-balance equations for a given flow geometry.

Case 1, Precursor Generation in Bulk

In this case, the precursor formation occurs exclusively in the bulk fluid; therefore, the rate of precursor generation is calculated by substituting the bulk temperature and concentrations in Equation 1. The second step depends upon whether the foulant formation takes place in the bulk fluid or at the interface. In case 1A, where the foulant formation occurs at the wall surface, transfer of soluble precursor to the interface is expressed in terms of the mass-transfer coefficient as shown below:

$$N_p = k_{mp}(C_{pb} - C_{pi}) \qquad (4)$$

The mass-transfer coefficient in the above equation is calculated by using the heat- and mass-transfer analogy . The rate of foulant formation is then expressed as follows:

$$r_f = \tilde{a}\, k_{2i}\, C_{pi}^{l} \qquad (5)$$

Where the parameter ã is used to convert the rate from a per-unit- volume to per-unit-surface-area basis, and k_{2i} is evaluated at the interface temperature.

In the model for Case 1B, Equation 2 is used to calculate the rate of foulant formation at the bulk temperature. The insoluble foulant is transported to the wall surface according to a mass-transfer equation, which is similar to Equation 4; however, the mass-transfer coefficient for the particle is calculated by using the following equation [4]:

$$k_m = v\,(f/8)^{1/2}/(11.8/Sc^{2/3}) \qquad (6)$$

The diffusion coefficient for particulate matter is calculated from the Stokes-Einstein equation.

$$D_p = 1.38\ 10^{-23}\ T/(3\,\pi\,\mu\,d_p) \qquad (7)$$

Case 2. Precursor Generation in Thermal-Boundary Layer

Two approaches may be taken to model the simultaneous mass transfer and reaction in the thermal boundary layer:

1. Using the film theory but allowing different film thicknesses for heat and mass transfer; and
2. Using the two-layer turbulent flow model, in which the turbulent-flow structures are modeled differently for the bulk and wall regions.

Although turbulent flow models are available, it is helpful to understand the overall fouling process by using the film theory first, so that the governing mechanism can be easily identified. The formulation of equations follows a procedure similar to that for the absorption of gases with simultaneous chemical reaction with appropriately modified boundary conditions. Applying the differential mass balance across a stagnant boundary layer and rearranging terms yields the following equation for reactant 1:

$$\rho_c \, D_{c1} \, \frac{d^2 C_{r1}}{d x^2} = k_1 \, Cr_1^{m} \, Cr_2^{n} \qquad (8)$$

Similar equations can be formulated for reactant 2 and precursor by incorporating appropriate stoichiometric constants for each reacting species. Temperatures and concentrations vary in the boundary layer; therefore, the coupled second-order equations are simultaneously solved with the boundary conditions stated below. Note that a linear temperature profile is used in the thermal-boundary layer; the heat of reaction is assumed to be negligible.

At the fluid/wall interface:

$$\frac{dC_{r1}}{dx} = \frac{dC_{r2}}{dx} = \frac{dC_p}{dx} = 0 \qquad (9)$$

At the edge of the diffusion-boundary layer C_{r1}, C_{r2}, C_p are equal to bulk values.

The thermal-boundary layer thickness was calculated as $\delta_T = k / h$.

The diffusion-boundary layer thickness for a given reacting species is calculated by using the heat- and mass-transfer analogy, as shown below for reactant 1:

$$\delta_{m1} = \delta_T(Pr/Sc_1)^{2/3} \qquad (10)$$

In the limiting case of Schmidt number >> Prandtl number, one can assume uniform temperature in the diffusion-boundary layer which serves to decouple the diffusion and reaction terms. On the other hand, one can assume negligible diffusion resistance, which gives a uniform concentration in the thermal-boundary layer. Paterson et al. (1988) used such an approach; however, in their analysis, they assumed zero-order reaction, and no distinction was made between the thermal- and momentum-boundary layers.

The set of equations represented by Equation 8 were solved and concentration profiles in the boundary layer for all components were determined. An iterative method was required to satisfy the boundary conditions at the edge of the boundary layer and at the interface. The calculated concentration profiles were used for calculation of an integrated rate of reaction and corresponding foulant formation in the boundary layer. The rate of deposition was assumed to be equal to the rate of foulant formed in the boundary layer. The integrated rate of reaction for each component is then incorporated into the mass balance calculation for that component.

Case 3. Precursor Generation at Wall

This is the simplest among the three fouling cases in terms of model development, and it was commonly used by prior investigators for a single-step reaction. Since both reactions are assumed to take place at the interface, reactants diffuse to the interface as shown below:

$$N_1 = k_{m1}(C_{r1b} - C_{r1i}) \qquad (11)$$

The reaction rate at the interface is expressed as follows:

$$r_1 = \tilde{a}\, k_{1i}\, C_{r1i}^{m}\, C_{ri2}^{n} \qquad (12)$$

A similar set of equations can be formulated for reactant 2. An expression representing generation of precursor, consumption, and back-diffusion is shown below:

$$\tilde{a}\ (\beta\, k_{1i}\, C_{r1i}^{m}\, C_{ri2}^{n} - k_{2i}\, C_{pi}^{l}) = k_{mp}(C_{pi} - C_{pb}) \qquad (13)$$

The set of nonlinear equations above is solved to determine the interfacial concentration, and hence the rate of foulant deposition. Note that the back-diffusion term plays an important role for determining the interfacial concentration.

EXPERIMENTAL ANALYSIS

Test Apparatus

Data are reported for experiments in two different fouling loops. The schematic flow diagram for the Argonne loop is shown in Figure 2. Fouling monitors are installed at inlet and outlet of the heating tube for measuring the fouling resistance at two different temperatures concurrently. The third fouling monitor is used for measuring the rate of deposition under near isothermal conditions (i.e., wall temperature within 5°C of the bulk temperature). The tube section is heated by boiling Dowtherm,® which in turn is heated by immersion electric heaters. The two fouling monitors can be maintained at the same wall temperature by adjusting the electric power. The test fluid is cooled in the reservoir by circulating coolant. Typically, 4-L of test fluid is used for a given experiment. The fouling monitor consists of a stainless-steel block installed on a tube section. Two sets of resistance-temperature devices (RTD) measure the temperature gradient in the block and the temperature difference between fluid and block. These two temperature-difference readings and the fluid temperature are used to calculate the heat-transfer coefficient and the interface temperature at a given time. The fouling resistance at a given time is then calculated as the difference in the heat-transfer resistance at that time and time $t = 0$.

The University of British Columbia loop [9] consists of a flow loop, in which an annular flow monitor is mounted. The fluid is circulated from a pressurized 9.5-L reservoir tank, which is initially heated by an immersion heater to bring the test fluid to the required temperature. The fluid in the tank is mixed by a motorized stirrer, and a cooling coil is used to maintain the fluid temperature. The annular monitor, supplied by Heat Transfer Research, Inc. (HTRI), consists of a resistance heater with four thermocouples located close to the heating surface. The change in the wall temperature is used for calculating the fouling resistance.

In both experiments, commercial odorless kerosene was used as a test fluid and indene was used to generate precursor. The fouling deposition consists of poly-peroxides produced by autoxidation of indene in the presence of dissolved oxygen. The fluid was saturated by purging with air at a given pressure. The fluid was then heated to the test condition, and the fouling test

was started. During the test period, constant air pressure was maintained by purging a small amount of air to keep the concentration of dissolved oxygen constant.

Application of Fouling Model

The rate equations formulated in the previous section are incorporated into the heat- and mass-balance equations in order to calculate the rate of fouling for the two apparatuses described above. The bulk concentrations of reactants and precursor are both space- and time-dependent for a closed-flow loop apparatus. Therefore, to avoid an elaborate numerical analysis, calculation of the fouling resistance as a function of time requires an assumption of quasi-steady-state conditions for an incremental time period. The simulation program used in the present investigation includes the following components: fouling monitor (two monitors for Argonne apparatus), flow tube, reservoir, and heating coil (for Argonne apparatus). The reservoir is treated as a well mixed reactor where generation of precursor takes place at the prevailing bulk temperature. For each time increment, a batch-reaction mode of calculation is applied to the reservoir for calculating the concentration of reactants and precursor for the next time increment by using the Runge-Kutta integration method. The fouling monitor, a test section, is treated as a tubular reactor, and corresponding heat- and mass-balance equations are used. Reaction in the isothermal tube section connecting the reservoir to the monitor is accounted for in the model. The heating coil in the Argonne apparatus is divided into n sections to calculate the local rate of fouling. However, in the present experiments, the heat flux was relatively low for the heating coil and no significant fouling was observed. In the next phase of the experimental program, heat fluxes that are comparable with those in the fouling monitors will be used in order to measure an overall rate of fouling for the heating coil.

RESULTS AND DISCUSSION

The objective of the present investigation was to evaluate the fouling model to identify the governing mechanisms of the fouling process. However, the fouling model contains several kinetic and physical constants that must be estimated. The kinetic constant A_1 for the first reaction between indene and oxygen was derived from the batch-reaction data of Russell [10]. Test conditions in Russell's experiment and the derived results are shown in Table 2. Note that Russell's data included only one temperature; therefore, the activation energy was estimated by using the oxidation data for styrene, for which the reaction mechanism was similar. On the basis of Russell's data on the solubility characteristics of indene poly-peroxide, it was assumed that foulant became insoluble for molecular number greater than 16. The corresponding molecular number for the precursor was assumed to be 4. Some variation (between 2 and 6) in the molecular number for precursor did not affect the overall results significantly. The chemistry of

the poly-peroxide formation by indene in the presence of dissolved oxygen, including the effects of selected solvents, is further studied by Wilson and Watkinson [11]. The density and thermal conductivity of the fouling film were assumed to be 1000 kg/m^3 and 0.2 W/m K, respectively. The film thermal conductivity was estimated by using the film-thickness measurement, and measured value of the fouling resistance.

Table 2. Test Conditions and Derived Results for Russell's Experiment

Reaction Conditions		
Reaction temperature	60	°C
Oxygen pressure	730	mm
Oxygen consumed	0.153	mol in 12 h
Indene (initial amount)	0.53	mol
Calculated Results		
Reaction order for indene	1.5	
Reaction order for oxygen	0.5	
Rate of reaction	0.0342	mol/hr L
Oxygen concentration	0.0086	mol/L
Indene concentration	8.35	mol/L
Activation energy	96.3	kJ/mol
Reaction constant A_1	$1.565\ 10^{10}$	(L/mol s)

The kinetic data for the second reaction are not available, so the fouling results were used to back-calculate the kinetic constant A_2. A set of baseline experiments at conditions shown in Table 3 were carried out in the Argonne and the University of British Columbia apparatus. Note that the fluid velocity for the University of British Columbia apparatus was slightly lower than that for the Argonne Apparatus; however, Reynolds numbers at the baseline conditions were comparable. The Case 2 model was run at average conditions for two sets of baseline Argonne data, and the kinetic constant A_2 was changed until the predicted fouling resistance at 14 h was comparable (see Figure 3). The activation energy was assumed to be the same as that for reaction 1. The resulting value of the kinetic constant A_2 was 1.1 x 10^8 1/s. For the Case 1A model, the conversion parameter ã (see Equation 5) for reaction 2 was estimated by following a similar procedure; the resulting value was 0.012, which corresponds to the ratio of the effective film thickness at the interface to the tube cross-sectional area. Both reactions take place at the interface in the Case 3 mechanism, and the corresponding value for the conversion parameter ã was 0.00021. Note that the conversion parameters for Cases 1A and 3 were not the same, because the basic assumptions used in both fouling mechanisms would not be simultaneously applicable to the experimental data. The uncertainty in the fouling-film properties and kinetic constant A_1 is lumped into the kinetic constant A_2 . The rate of fouling is independent of wall temperature for the Case 1B mechanism, and the in-tube monitor used to determine the

isothermal fouling rate did not measure any detectable fouling for test conditions used in the present investigation. It was concluded that the experimental data did not follow the Case 1B mechanism; therefore, no further analysis for this model was carried out.

Table 3. Baseline Test Conditions

Argonne National Laboratory		
Fluid velocity	1.06	m/s
Bulk temperature	83	°C
Interface temperature	192	°C
Indene concentration	10%	by weight
Air pressure	420	kPa
University of British Columbia		
Fluid velocity	0.61	m/s
Bulk temperature	82	°C
Interface temperature	188	°C
Indene concentration	10%	by weight
Air pressure	410	kPa

The experimental results in Figure 3 show an increasing rate of fouling with time. The predicted results indicate that the observed fouling trend was mostly due to an increase in the precursor concentration with time. The Case 1A and Case 2 models predicted the fouling trend with a reasonable accuracy; however, the Case 3 model predicted a nearly linear fouling, which can be explained as follows. The interfacial temperature for a given test run was maintained constant, and the prediction of the Case 3 model depends strongly upon the interfacial temperature. The bulk reaction is not included, and the precursor buildup in the bulk by back diffusion of precursor is relatively low. As a result, the rate of deposition was nearly constant, giving a linear fouling trend. On the other hand, the Case 1A and Case 2 models account for the bulk reaction, allowing precursor concentration to vary with time. Both models also allow the bulk reaction to occur not only in the fouling monitor but also in the reservoir and flow sections of the closed-flow-loop apparatus.

Effects of Physical Parameters

The Argonne experiments were conducted with an in-tube flow monitor, while the University of British Columbia used an annular flow monitor. The effects of flow passage and prediction capability of the fouling model were determined by comparing the two sets of fouling data obtained at comparable conditions. The bulk temperature was comparable; however, the interfacial temperature and fluid velocity for the annular monitor were slightly lower than those for the in-tube monitor (see Table 3). Figures 4, 5, and 6 show comparisons of the fouling trend for the two monitors and predictions by the three models. The fouling resistance for the annular monitor was comparable with that for the in-tube monitor for about the first 10 hours, after which

the rate of fouling for the annular monitor was higher than that for the in-tube monitor. The Case 1A model predicted a significantly higher rate of fouling than was obtained in the experimental data for the annular monitor. The Case 2 model predicted the annular-monitor data more accurately than did the other two models, which indicated that the Case 2 model should be used for applying the experimental data for a given flow geometry to another geometry. Since the interface temperature for the annular monitor was slightly lower than that for the in-tube monitor, the fouling resistance predicted by the Case 3 model was lower for the annular monitor than that for the in-tube monitor. In summary, the results showed that the Case 2 fouling model predicted the effects of fluid dynamics in two flow geometries more accurately than did the other two models.

The effects of the interfacial temperature on the rate of fouling and the predicted results from the three models are shown in Figures 7, 8, and 9 for the annular-monitor experiments. The two sets of fouling data were obtained at the interfacial temperatures of 188 and 133°C. Other parameters were kept at the baseline conditions shown in Table 3. The rate of fouling predicted by the Case 1A model was higher than that obtained in the experimental data for both interfacial temperatures, but the fouling trend agreed within reasonable accuracy. The Case 2 model was able to predict the effects of the interfacial temperature more accurately than were the other two models, as shown in Figure 8. As discussed earlier, the predicted fouling resistance was linear in time for the Case 3 model and was lower than the experimental data. Note that the fouling resistance predicted by the Case 3 model was negligibly small for the interfacial temperature of 133°C, which indicates that no significant fouling would have occurred for an extended period. The present set of data show that the case 2 model should predict the effects of interfacial temperature (i.e., heat flux) on the rate of fouling more accurately than the other two models; however, the case 1A model would predict the fouling trend with reasonable accuracy.

The effects of bulk temperature on the rate of fouling are shown in Figures 10, 11, and 12 for the in-tube fouling monitor, together with the predicted results for Cases 1A, 2, and 3, respectively. The interfacial temperature ($188 \pm 4^{o}C$) and fluid velocity ($1.06 \pm .05$ m/s) for the three test runs were kept nearly constant; therefore, the observed rate of fouling showed the effects of generation of precursor at the bulk temperature. Both the Case 1A and Case 2 models predicted the effects of the bulk temperature more accurately than did the Case 3 model; however, the Case 2 model prediction was closer to the experimental data than was the case 1A model prediction. The bulk reaction is neglected in the Case 3 model; therefore, the predicted rate of fouling stayed nearly the same for the three bulk temperatures. The predicted results and the experimental data clearly showed that the bulk temperature should be considered along with

the interfacial temperature in analyzing the effects of temperature on the rate of fouling, unless it is shown that the fouling process is controlled entirely by the Case 3 mechanism. This observation is quite important in the application of the experimental data obtained with a closed-flow-loop apparatus to industrial conditions. A fouling model that predicts the combined effects of the bulk and interfacial temperatures should be employed in applying the experimental data to industrial conditions. The level of uncertainty associated with the commonly used method of correlating the fouling rate with the interfacial temperature and calculating the corresponding activation energy is unknown.

CONCLUSIONS

An analytical model was developed to identify the basic mechanisms governing the overall fouling process. On the basis of the analytical and experimental results, the following conclusions can be stated. In the next phase of the analytical work, the fouling model will be validated by comparing the predicted rate of fouling (slope of fouling resistance vs. time) with the new set of experimental data.

1. A fouling model, even though it may be approximate, can serve as a useful tool for analysis of the experimental data. Such an analytical tool is required for identifying the controlling mechanism(s) in the overall fouling process, determining the effects of physical conditions, and applying the experimental data to industrial conditions.
2. The experimental data showed a trend of increasing fouling rate with time. Such a fouling trend was expected for a closed-flow-loop apparatus. This conclusion was supported by the predicted results obtained with the Case 1A and Case 2 fouling models, in which the bulk reaction was included.
3. The Case 2 model predicted the results obtained with the annular flow monitor more accurately than did the other models, after their validation with the experimental data for the in-tube monitor. This shows that the Case 2 model most correctly represented the fluid dynamics for the present set of conditions.

ACKNOWLEDGMENTS

The authors wish to thank Dr. G. Zhang for conducting experiments at the University of British Columbia, and Mr. J. Falkenberg for conducting experiments at Argonne.

NOMENCLATURE

â	parameter in Equation 5	(m^3/m^2)
A_1	kinetic constant for reaction 1	(m^3/kmol s)
A_2	kinetic constant for reaction 2	(1/s)
C	concentration	(kmol/m^3)
D_c	diffusivity of dissolved component	(m^2/s)
D_p	diffusivity of particulate matter	(m^2/s)
d_p	particulate diameter	(m)
E	activation energy	(kJ/kmol)
f	friction factor	
h	heat-transfer coefficient	(kW/m^2 K)
k	thermal conductivity	(kW/m K)
k_m	mass-transfer coefficient	(m/s)
N	mass flux	(kmol/m^2 s)
Pr	Prandtl number	
r	reaction rate	(kmol/m^3 s)
R	gas constant	(kJ/kmol K)
Sc	Schmidt number	
T	temperature	(K)
v	fluid velocity	(m/s)
x	x coordinate in boundary layer	(m)
β	stoichiometric parameter	
δ_T	thermal-boundary-layer thickness	(m)
δ_m	diffusion-boundary-layer thickness	(m)
μ	viscosity	(Pa s)
ρ_c	density	(kmol/m^3)

subscripts

b	bulk
i	interface
f	foulant
p	precursor
r1	reactant 1
r2	reactant 2

superscripts

m reaction order for reactant 1

n reaction order for reactant 2

l reaction order for precursor

REFERENCES

1. Watkinson, A. P., *Critical Review of Organic-Fluid Fouling*, Argonne National Laboratory Report, ANL/CNSV-TM-208 (1988).

2. Kern, D. Q., and R. E. Seaton, *Brit. Chem. Eng.*, Vol. 4, 258-262 (1959).

3. Crittenden, B. D., *Fouling Science and Technology*, (Melo, Bott, and Bernardo, eds.), p. 293 NATO ASI Series 145, Kluwer Academic Publishers, Boston, (1988).

4. Nijsing, R., 1964, *Diffusional and kinetic phenomena associated with fouling*, Euratom Report, EUR 543.

5. Watkinson, A. P., and N. Epstein, *Proc. 4th Int. Heat Transfer Conf.*, Paris, Vol. 1, Paper 1.6 (1970).

6. Crittenden, B. D., S. T. Kolaczkowski, and S.A. Hout, *Inst. of Chem. Eng. Res. Des.*, Vol. 65, 171-179 (1987).

7. Paterson, W. R., and P. J. Fryer, *Chem. Eng. Sci.*, Vol. 43, No. 7, 1714-1717 (1988).

8. Himmelblau, D.M., and K.B. Bishoff, *Process Analysis and Simulation,* Wiley and Sons, Chapter 2 (1968).

9. Asomaning, S., and A. P. Watkinson, *Can. J. Chem. Eng.*, Vol. 70, 444-451 (1992).

10. Russell, G. A., *J. Am. Chem. Soc.*, Vol. 79, 1035-1040 (1956).

11. Wilson, D.I., and A.P. Watkinson, *Heat Transfer - 3rd U.K. Nat'l. Conf. Inst. Chem. Eng.*, Vol. 2, 987-994 (1992).

DATE
FILMED
11/4/93
END